Manipulating Semiconductor Colloidal Stability Through Doping

Mark E. Fleharty,[1,2] Frank van Swol,[2,3,*] and Dimiter N. Petsev[2,†]
[1]Nanoscience and Microsystems Program, University of New Mexico, Albuquerque, New Mexico 87131, USA
[2]Department of Chemical and Biological Engineering, University of New Mexico, Albuquerque, New Mexico 87131, USA
[3]Sandia National Laboratories, Albuquerque, New Mexico 87185, USA
(Received 10 June 2014; published 7 October 2014)

The interface between a doped semiconductor material and electrolyte solution is of considerable fundamental interest, and is relevant to systems of practical importance. Both adjacent domains contain mobile charges, which respond to potential variations. This is exploited to design electronic and optoelectronic sensors, and other enabling semiconductor colloidal materials. We show that the charge mobility in both phases leads to a new type of interaction between semiconductor colloids suspended in aqueous electrolyte solutions. This interaction is due to the electrostatic response of the semiconductor interior to disturbances in the external field upon the approach of two particles. The electrostatic repulsion between two charged colloids is reduced from the one governed by the charged groups present at the particles surfaces. This type of interaction is unique to semiconductor particles and may have a substantial effect on the suspension dynamics and stability.

DOI: 10.1103/PhysRevLett.113.158302 PACS numbers: 82.70.Dd, 73.40.Mr

Semiconductor colloids are of significant fundamental interest and present opportunities for new and exciting applications [1,2]. A basic property pertinent to any colloidal system is its stability. Semiconductor colloids are no different. Strategies to stabilize such systems employ electrostatic and/or steric [3,4] repulsion against van der Waals attraction to prevent the particles from coagulating. The balance between electrostatic repulsion and van der Waals attraction is the foundation of the celebrated Derjaguin-Landau-Verwey-Overbeek (DLVO) theory of colloid stability [5,6]. We find that the charge density in the doped semiconductor particle interior plays an essential role and can significantly alter the overall interaction. It has been experimentally established that the charge density inside a doped semiconductor in the vicinity of a semiconductor-electrolyte interface will shift in response to changes in the electrostatic potential in the electrolyte phase. This effect has been exploited to perform force measurements [7,8] and is utilized in a significant number of sensing applications that use nanoscale semiconductors [9–13].

We hypothesize that the internal charge redistribution due to external field perturbation should in turn affect the force between two approaching semiconductor colloidal particles. Hence, the DLVO theory has to be revisited when applied to doped semiconductor colloids. In this Letter we provide such a revision based on a general electrostatic analysis. We show that the internal response of the doped semiconductor particles to changes of the potential in the electrolyte may have a dramatic effect on their kinetic stability. In addition, it opens up possibilities of new methods for control and manipulation.

The system under consideration consists of two spherical colloidal particles suspended in an electrolyte solution. In order to be specific, let the particles have Si cores (other semiconductors will perform similarly) and the terminal ligands at the surface have $-SiO^-$ groups [3]. Such oxide layer may naturally form when Si is exposed to air or water that has dissolved oxygen. The $-SiO^-$ groups are subject to surface charge regulation [14–16] through chemical equilibria with constants K_- and K_+ such that

$$\begin{aligned} SiOH_2^+ &\rightleftharpoons SiOH + H^+, \qquad pK_+ = -\log_{10}K_+, \\ SiOH &\rightleftharpoons SiO^- + H^+, \qquad pK_- = -\log_{10}K_-. \end{aligned} \tag{1}$$

We will assume (without loss of generality) that the cores are n-doped. The potential Ψ in the two domains is described by the Poisson equation [17]

$$\nabla^2\Psi = -\frac{\rho}{\epsilon\epsilon_0}, \tag{2}$$

where ρ is the charge density, and ε and ε_0 are the medium dielectric permittivity and the dielectric constant of vacuum, respectively. The charge density in the electrolyte solution is distributed according to Boltzmann's classical statistical mechanics. In contrast, the charge distribution density in the doped semiconductor particle core is subject to quantum exclusion limitations and may have to be described by a temperature dependent Fermi-Dirac distribution [18,19]. The charge densities are given as

$$\rho = \begin{cases} \sum_i n_i^0 z_i \exp\left(\frac{-z_i e\Psi}{k_B T}\right), & \text{electrolyte} \\ eN_d\left[1 - \chi F_{1/2}\left(\frac{\mu - e\Psi}{k_B T}\right)\right], & \text{semiconductor} \\ 0, & \text{oxide,} \end{cases} \tag{3}$$

where e is the fundamental unit of charge, k_BT is the thermal energy, n_i^0 is the bulk number density of species i, z_i is the charge of ion i, N_d is the number density of donors in the semiconductor, and $\hbar$ is the reduced Planck constant. $F_{1/2}$ is the Fermi integral and is defined as

$$F_{1/2}(x) = \frac{2}{\sqrt{\pi}} \int_0^\infty dt \frac{t^{1/2}}{1 + \exp(t - x)}, \tag{4}$$

where μ is the Fermi level [19], and the parameter χ is given by

$$\chi = \frac{1}{4N_d} \left(\frac{2m^* k_B T}{\pi \hbar^2} \right)^{3/2}, \tag{5}$$

where m^* is the effective mass of the electron. The charge density inside the oxide layer is zero.

Since we are considering a system at room temperature, it is appropriate to use the limiting case of the Fermi function where

$$\chi F_{1/2}\left(\frac{\mu - e\Psi}{k_B T} \right) \to \exp\left(-\frac{e\Psi}{k_B T} \right). \tag{6}$$

The boundary conditions required to solve Eq. (2), are to match potentials at the interfaces of the semiconductor (subscript "sc"), oxide (subscript "ox") and electrolyte (subscript "el") such that the charge regulating boundary condition is enforced at the oxide-electrolyte interface through

$$\Psi_{\rm ox} = \Psi_{\rm el} = \Psi_s; \qquad \sigma_s = \mathbf{n} \cdot [\varepsilon_{\rm ox} (\nabla \Psi)_{\rm ox} - \varepsilon_{\rm el} (\nabla \Psi)_{\rm el}] \tag{7}$$

while the boundary conditions applied at the semiconductor-oxide interface are

$$\Psi_{\rm sc} = \Psi_{\rm ox}; \qquad 0 = \mathbf{n} \cdot [\varepsilon_{\rm sc} (\nabla \Psi)_{\rm sc} - \varepsilon_{\rm ox} (\nabla \Psi)_{\rm ox}], \tag{8}$$

where σ_s and Ψ_s are the surface charge and potential governed by the chemical equilibria given in Eq. (1), $\mathbf{n}$ is the vector normal to the surface, and $\epsilon_{\rm sc}$, $\epsilon_{\rm ox}$, $\epsilon_{\rm el}$ are the dielectric constants of the semiconductor, oxide, and electrolyte, respectively.

In this model we use a site dissociation model such that the charge density is given by [14,20]

$$\sigma_s(\Psi_s) = \frac{e\Gamma\delta \sinh[e(\Psi_N - \Psi_s)/k_B T]}{1 + \delta \cosh[e(\Psi_N - \Psi_s)/k_B T]}. \tag{9}$$

Γ is the number of ionizable groups per unit area at the surface, $\delta = 2\sqrt{K_-/K_+}$, Ψ_s is the potential at the solid-liquid interface [see Eq. (7)], the Nernst potential Ψ_N is given as

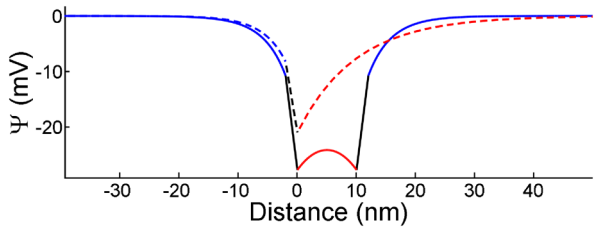

FIG. 1 (color online). One-dimensional potential distributions in the electrolyte solution (red), oxide layer (black), and the semiconductor (blue) approximated as infinite flat plates. The solid line corresponds to two particles separated by 10 nm, while the dashed line corresponds to the potential distribution of a single particle in isolation. These curves illustrate how the potential distribution inside the semiconductor responds to the presence of an approaching colloid. The particles are covered with $-\mathrm{SiO}^-$ groups with surface density $\Gamma = 8 \times 10^{18}$ m^{-2}. These groups may release or attach a proton according to Eq. (1). The parameters for this calculation are $p\mathrm{H} = 3.5$, the overall electrolyte concentration is 0.925 mM (adjusted by adding a symmetric monovalent electrolyte), $p\mathrm{K}_+ = -2$, $p\mathrm{K}_- = 6$, and the particle doping is 10^{24} m^{-3}. The dielectric permitivities were $\varepsilon_{\rm el} = 78.5$ for the electrolyte, $\varepsilon_{\rm sc} = 11.7$ for Si, and $\varepsilon_{\rm ox} = 3.9$ for the 2 nm thick layer of SiO_2 [22,23].

$$\Psi_N = \frac{k_B T}{e} \ln(10)(p\mathrm{I} - p\mathrm{H}), \tag{10}$$

the isoelectric point is given as $p\mathrm{I} = (p\mathrm{K}_+ + p\mathrm{K}_-)/2$, $p\mathrm{H}$ denotes the value for the $p\mathrm{H}$ far from the interface and $p\mathrm{I}$ is the isoelectric point of the solid-liquid interface.

The spatial dependence of the electrostatic potential Ψ and charge density ρ on the distance between two particles with a separation of 10 nm and a particle in isolation is shown in Fig. 1. The results presented in the figure were obtained by numerically solving Eqs. (2) and (3). Alternatively, the exact analytical solution of Behrens and Borkovec for interacting surfaces with charge regulation [21] can be adapted to obtain the same results. As the distance between the charged particles varies, the potential distribution changes in the electrolyte filled gap between the surfaces as well as in the particle interior. This is due to the fact that the potentials inside and outside of the particles are connected through Eqs. (7) and (8). The coupling goes both ways; hence, the potential and charge distributions in the electrolyte will be affected by the fact that the inner charges respond by internal redistribution to the particle approach.

Knowing the effect of separation on the potential and charge density distributions, in both the particle interior and exterior, allows us to derive the pair electrostatic energy of interaction between the two spherical colloidal particles of radius a separated by distance h using the Derjaguin method [5,6]

$$U_e(h) = \pi a \int_h^\infty dy \int_\infty^y dz \Pi_e(z), \tag{11}$$

where y and z are distance variables. A detailed description of the solution and the assumptions made is given in Supplemental Material [24], but we should emphasize here that the pressure Π_e depends on the electrostatic potentials, and hence on the separation distance. The total energy of interaction consists of [5,6]

$$U(h) = U_e(h) + U_{\mathrm{vdw}}(h) \tag{12}$$

with U_{vdw} being the van der Waals attractive energy, which for small separations is $U_{\mathrm{vdw}}(h) = A_H a/12h$, where A_H is the Hamaker constant [5,6,25].

The total interaction energy given by Eq. (12) is shown in Fig. 2. The height of the maximum determines the stability against coagulation. Overcoming the barrier brings the two particles into the region of very close separations where the van der Waals attraction completely overpowers the electrostatic repulsion and leads to irreversible coagulation. The difference between the energy maxima for doped and undoped semiconductor colloids and the parameters listed in Figs. 1 and 2 is slightly more than 4 k_BT. It is due to the fact that the internal charge density redistribution in the doped semiconductor reduces the potential in the electrolyte gap between the particle surfaces. Hence, the electrostatic repulsion for doped particles is less than that for undoped particles, which leads to a different energy curve (see Fig. 2). The inset shows the energy change that is due to the doping. This is a new type of colloidal interaction that is uniquely characteristic of semiconductor colloids in aqueous suspension and is very significant in both magnitude and range. This effect depends on the doping concentration and decreases as the latter goes down and vice versa.

Suspensions characterized by a combination of van der Waals and electrostatic interactions are thermodynamically unstable and, given enough time, will ultimately coagulate. The energy barrier, however, provides kinetic stability that may allow for sufficient time for different applications and processing. The rate equation describing the coagulation of two colloidal particles (formation of doublets) is [26–28]

$$\frac{dn_2}{dt} = k_c n_1^2, \tag{13}$$

where n_2 is the concentration of coagulated pairs (doublets), n_1 is the concentration of single particles, t denotes time, and $k_c = k_0/W$ is the rate constant.

With k_0 we denote the rate constant in the absence of any long range interactions and energy barriers (the rate is purely diffusion limited). The effect of slowing down due to the presence of an energy barrier is taken into account by the stability factor [28–30]

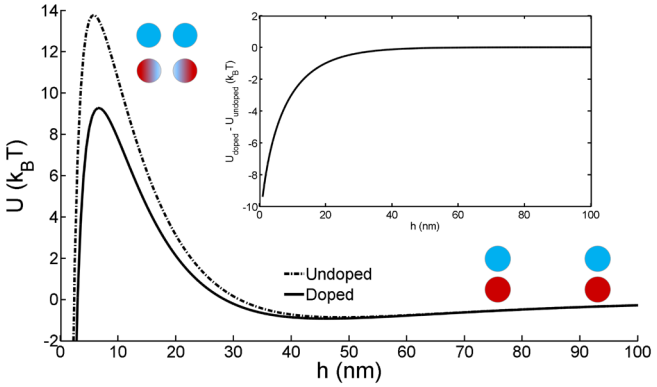

FIG. 2 (color online). Interaction between colloids. Interaction energy between undoped (blue particles, full line) and doped (red particles, dashed line) semiconductor colloids. As the particles approach the charge density in the doped particles redistribute. which is illustrated by the gradual color change. The Hamaker constant used to generate these plots is $A_H = 5.4 \times 10^{-20}$ J, and the particle radius is $a = 100$ nm. The rest of the parameters are the same as in Fig. 1. The inset shows the difference between the two energy curves.

$$W = 4a \int_0^\infty \frac{H(h)\exp[U(h)/k_BT]}{h - 2a}\, dh, \tag{14}$$

where $H(h) = (4h + a)/4h$ embodies the hydrodynamic effects [31], also see the Supplemental Material [24].

For the parameters in Figs. 1 and 2, the coagulation rate in an undoped sample will be more than 60 times slower than in the doped sample (see Fig. 3). This is a significant difference that cannot be ascertained using the conventional DLVO theory. This new effect is entirely due the internal mobility and reconfiguration of charges in the doped semiconductor. Figure 3(a) illustrates how the stability factor W of the colloidal system depends on doping [see Eq. (14)]. The relative coagulation rate is shown in the inset. As the doping level increases, the doped system becomes more unstable and prone to coagulation and precipitation. Figure 3(b) illustrates how a change in the ionic concentration affects the stability of the colloids.

In the limit where the surface potential is small, $|\Psi_s| <$ 26 mV we have derived Eq. (15) for the surface potential (see also the Supplemental Material [24])

$$\Psi_s = \frac{\Gamma\delta e \sinh(e\Psi_N/k_BT)}{[\delta\cosh(e\Psi_N/k_BT) + 1]\left[\epsilon_0\epsilon_{\mathrm{el}}\kappa_{\mathrm{el}}\tanh(\frac{\kappa_{\mathrm{el}}h}{2}) + \frac{\epsilon_0\epsilon_{\mathrm{ox}}\epsilon_{\mathrm{sc}}\kappa_{\mathrm{sc}}}{\epsilon_0 + L_{\mathrm{ox}}\epsilon_{\mathrm{sc}}\kappa_{\mathrm{sc}}} + \frac{\Gamma\delta e^2[\cosh(e\Psi_N/k_BT)+\delta]}{k_BT[\delta\cosh(e\Psi_N/k_BT)+1]^2}\right]}. \tag{15}$$

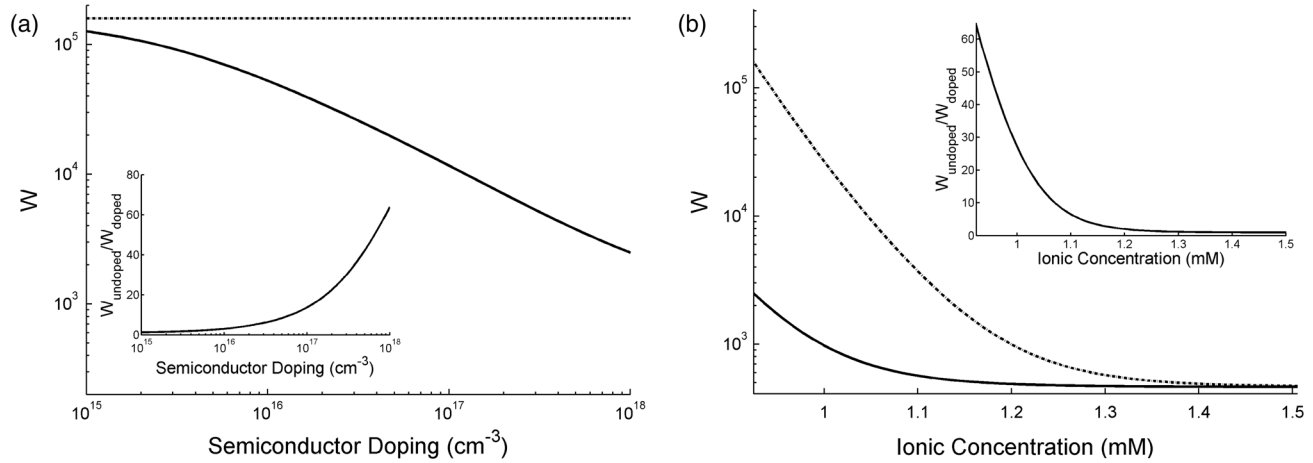

FIG. 3. Differences in stability due to doping. (a) Stability of undoped (dashed) and doped colloids (solid) versus semiconductor doping concentration. The stabilities are useful for calculating the time to coagulation. The inset shows the relative stability $W_{\mathrm{undoped}}/W_{\mathrm{doped}}$ versus doping. The relative stability is useful for calculating the relative times to coagulation for undoped versus doped particles. (b) Stability of undoped (dashed) and doped colloids (solid) versus the ionic concentration of the electrolyte. The relative stability $W_{\mathrm{undoped}}/W_{\mathrm{doped}}$ versus the ionic concentration of the electrolyte is given in the inset. The rest of the parameters are the same as in Figs. 1 and 2.

The inverse Debye lengths are given as $\kappa_{\mathrm{sc}} = \sqrt{n_{\mathrm{sc}}e^2/\epsilon_{\mathrm{sc}}\epsilon_0 k_B T}$ and $\kappa_{\mathrm{el}} = \sqrt{n_{\mathrm{el}}e^2/\epsilon_{\mathrm{el}}\epsilon_0 k_B T}$ for the semiconductor and electrolyte phases, respectively, where n_{sc} and n_{el} are the number densities of ions, also for the semiconductor and electrolyte phases, respectively. Equation (15) allows for the derivation of analytical expressions for the potential distributions in all phases. Further analysis provides insight into the functional form of the surface potential in various limits. In the low doping limit, $\kappa_{\mathrm{sc}} \to 0$, we recover the equivalent expression for charge regulation at a dielectric-electrolyte interface. Similarly, when the thickness of the oxide L_{ox} is large such that $L_{\mathrm{ox}} \to \infty$ we again recover the expression for charge regulation at a dielectric-electrolyte interface. In the high doping, or metal-like, limit where $\kappa_{\mathrm{sc}} \to \infty$ and $L_{\mathrm{ox}} \to 0$ the effect from the redistribution of charges in the semiconductor region is even stronger, as long as there is an oxide barrier to prevent the release of ions into solution. In the case of a metal-like particle without an oxide, the charge regulation formulas would have to be revisited.

The internal mobility of the charges (electrons and/or holes) in semiconductor materials has been experimentally demonstrated and utilized in different sensing applications [1,2,7–12,32–34]. In this Letter, we used first principle continuum electrostatics [17] to develop a simple model that allows one to find the effect of the internal charge mobility on the external potential distribution and hence on the electrostatic interaction between two approaching colloidal spheres. The internal charge redistribution manifests itself as a reduction of the electrostatic repulsion (or alternatively can be defined as an apparent additional attractive contribution to the energy, see the inset in Fig. 2). While one may think that this interaction is similar to the van der Waals attraction, the truth is that it has a very different functional dependence on separation. Instead of following a power law it decays almost exponentially, which is due to its electrostatic origin. It is very interesting that the effect of the reduction in the electrostatic repulsion is primarily dependent on the doping level and much less on whether the semiconductor particles are n-doped, p doped, or mixed. In addition to the n-doped particle interaction (the dashed line in Fig. 2) we have computed the interaction potentials between p-doped particles as well as that between an n-doped and a p-doped particle. All these curves practically collapse onto a single one, which is almost indistinguishable from the dashed curve in Fig. 2. This means that the main reason for the observed effect is that there is a dynamically responsive charged fluid in the particle interior that responds to potential perturbations. The polarity of the inner charges is practically unimportant.

The surface chemistry plays a key role in determining the strength of the interaction between semiconductor dopants and the electric double layer. The difference between the chemical equilibria constants, $\Delta p\mathrm{K} = p\mathrm{K}_- - p\mathrm{K}_+$, determines the strength of the charge regulation at the interface [35]. A large $\Delta p\mathrm{K}$ allows for larger changes in the surface potential as the distance h is varied. Particle surfaces with a low $\Delta p\mathrm{K}$ would show little change in stability with doping, while surfaces with a large $\Delta p\mathrm{K}$ (i.e., silica, $\Delta p\mathrm{K} = 8$) allow for relatively large changes in surface potential and hence exhibit large changes in stability due to doping.

The new type of interaction that we have identified has significant implications on the processing and handling of semiconductor colloids. The first obvious conclusion is that doped colloids will be less stable and much more prone to coagulation than their undoped counterparts. Figure 3 gives an idea about the relative time windows for kinetic stability. As mentioned above, the average lifetime for a suspension of silicon colloid with a $10^{18}/\mathrm{cm}^3$ doping level will be more than 60 times shorter than that for an undoped sample

with the same surface chemistry. This effect can be exploited to separate doped from undoped particles in aqueous suspensions, or even sort the particles based on their doping. Heavily doped particles will precipitate faster and can be separated from the rest by simple filtration or centrifugation. They then can be redispersed using sonication. The procedure can be repeated multiple times to obtain particles with a narrow distribution of the doping levels.

Increasing the *p*H beyond the isoelectric point leads to an increase in the value of the surface potential and hence to an increase in the repulsion and stability of the suspension. Similar will be the effect of reducing the background electrolyte concentration, which will extend the range of the overall electrostatic repulsion. Colloidal suspensions can be used to fabricate ordered crystal-like structures that have excellent properties for photonic applications [36]. Figure 2 implies that among other things the particle doping may have an effect on the spacing and ordering in crystals composed of semiconductor colloidal particles. Doped particles will be spaced on the average closer than undoped particles. For example, a close inspection of the energy curves in Fig. 2 show that the average spacing of the doped particles will be about 2 nm smaller than that for the undoped particles. We are convinced that a better understanding of the interface between semiconductor materials and electrolyte solutions will be instrumental in the effort to design novel "smart" materials at the micro- and nanoscale.

This research is supported by NSF (CBET 0844645) and the United States Department of Energy, Office of Basic Energy Sciences, Division of Materials Sciences and Engineering. Sandia National Laboratories is a multiprogram laboratory managed and operated by Sandia Corporation, a wholly owned subsidiary of Lockheed Martin Corporation, for the U.S. Department of Energy's National Nuclear Security Administration under Contract No. DE-AC04-94AL85000.

*fbvansw@sandia.gov
†dimiter@unm.edu

[1] D. V. Talapin, J.-S. Lee, M. V. Kovalenko, and E. V. Shevchenko, Chem. Rev. **110**, 389 (2010).
[2] F. Meseguer, R. Fenollosa, I. Rodriguez, E. Xifré-Perez, F. Ramiro-Manzano, M. Garín, and M. Tymczenko, J. Appl. Phys. **109**, 102424 (2011).
[3] A. Nag, M. V. Kovalenko, J.-S. Lee, W. Liu, B. Sokoyny, and D. V. Talapin, J. Am. Chem. Soc. **133**, 10612 (2011).
[4] L. M. Wheeler, N. R. Neale, T. Chen, and U. R. Kortshagen, Nat. Commun. **4**, 1 (2013).
[5] E. J. W. Verwey and J. T. G. Overbeek, *Theory of the Stability of Lyophobic Colloids* (Elsevier, New York, 1948).
[6] B. V. Derjaguin, N. V. Churaev, and V. M. Muller, *Surface Forces* (Plenum, New York, 1987).
[7] E. Greenfield and U. Sivan, Phys. Rev. Lett. **102**, 106101 (2009).
[8] S. Lekkala, J. A. Marohn, and R. F. Loring, J. Chem. Phys. **139**, 184702 (2013).
[9] Y. Cui, Q. Wei, H. Park, and C. M. Lieber, Science **293**, 1289 (2001).
[10] J.-L. Hahm and C. M. Lieber, Nano Lett. **4**, 51 (2004).
[11] F. Patolsky, B. P. Timko, G. Yu, Y. Fang, A. B. Greytak, G. Zheng, and C. M. Lieber, Science **313**, 1100 (2006).
[12] F. Patolsky, G. Zheng, O. Hayden, M. Lakadamyali, X. Zhuang, and C. M. Lieber, Proc. Natl. Acad. Sci. U.S.A. **101**, 14017 (2004).
[13] Y. Zhang, T. C. Gamble, A. Neumann, G. P. Lopez, S. R. Brueck, and D. N. Petsev, Lab Chip **8**, 1671 (2008).
[14] B. W. Ninham and V. A. Parsegian, J. Theor. Biol. **31**, 405 (1971).
[15] S. H. Behrens and M. Borkovec, J. Chem. Phys. **111**, 382 (1999).
[16] S. L. Carnie and D. Y. C. Chan, J. Colloid Interface Sci. **161**, 260 (1993).
[17] L. D. Landau and E. M. Lifshitz, *Electrodynamics of Continuous Media* (Nauka, Moscow, 1982).
[18] R. Kubo, *Statistical Mechanics, an Advanced Course with Problems and Solutions* (North-Holland, Amsterdam, 2004).
[19] R. P. Feynman, N. Metropolis, and E. Teller, Phys. Rev. **75**, 1561 (1949).
[20] D. Y. C. Chan, T. W. Healy, and L. R. White, J. Chem. Soc., Faraday Trans. 1 **72**, 2844 (1976).
[21] S. H. Behrens and M. Borkovec, Phys. Rev. E **60**, 7040 (1999).
[22] J. N. Israelachvili, *Intermolecular and Surface Forces.* 2nd ed. (Academic, New York, 2011).
[23] J. Fritz, E. B. Cooper, S. Gaudet, P. K. Sorge, and S. R. Manalis, Proc. Natl. Acad. Sci. U.S.A. **110**, 389 (2010).
[24] See Supplemental Material at http://link.aps.org/supplemental/10.1103/PhysRevLett.113.158302 for [brief description].
[25] H. C. Hamaker, Physica (Amsterdam) **4**, 1058 (1937).
[26] R. M. Mazo, *Brownian Motion: Fluctuations, Dynamics and Applications* (Clarendon, Oxford, 1937), Vol. 112.
[27] M. von Smoluchowski, Ann. Phys. (Berlin) **326**, 756 (1906).
[28] W. B. Russel, D. A. Saville, and W. R. Schowalter, *Colloidal Dispersions* (Cambridge University Press, Cambridge, England, 1989).
[29] P. M. Debye, Trans. Electrochem. Soc. **82**, 265 (1942).
[30] N. A. Fuchs, Z. Phys., 736 (1934) (in German).
[31] B. V. Derjaguin and V. M. Muller, Dokl. Akad. Nauk SSSR **176**, 738 (1967) (in Russian).
[32] J. M. Rothberg, W. Hinz, T. M. Rearick, J. Scultz, W. Mileski, M. Davey, J. H. Leamon, K. Johnson, M. J. Milgrew, M. Edwards *et al.*, Nature (London) **475**, 348 (2011).
[33] G. Zheng, F. Patolsky, Y. Cui, W. U. Wang, and C. M. Lieber, Nat. Biotechnol. **23**, 1294 (2005).
[34] L. Shi, J. T. Harris, R. Fenollosa, I. Rodriguez, X. Lu, B. A. Korgel, and F. Meseguer, Nat. Commun. **4**, 1 (2013).
[35] R. Ettelaie and R. Buscall, Adv. Colloid Interface Sci. **61**, 131 (1995).
[36] S.-H. Kim, S. Y. Lee, S.-M. Yang, and G.-R. Yi, NPG Asia Mater. **3**, 25 (2011).